Fig. 2. Positional cloning of the dfk mutation. A: distribution of haplotypes observed among 22 dfk-homozygous F2 progeny carrying a recombinant chromosome between D1Rat133 and D1Rat295. White boxes, homozygote for the WTC allele. Grey boxes, heterozygote. Black boxes, homozygote for the ACI allele. B: dfk was genetically mapped to 0.8-cM region between D1Kyo9 and D1Mgh10. The dfk showed no recombination with D1Wox9 in 480 informative meioses. The dfk locus was physically localized to the ~1-Mb region defined with D1Kyo9 and D1Mgh10. Within the dfk locus, 4 genes have been mapped. In the WTC-dfk rats, a genomic sequence containing Kcnq1 exon 7 was deleted. The 5'- and 3'-breakpoints of the deleted sequence are indicated by arrowheads. C: expression of Kcnq1 assessed by Northern blot analysis. Poly(A) RNAs from the hearts of WTC and WTC-dfk rats are hybridized with a probe containing exons 9–14 of rat Kcnq1. A smaller Kcnq1 transcript due to the loss of exon 7 was observed in WTC-dfk. Hybridization signals of β-actin on the same blot are shown at bottom. Molecular weight markers are indicated to the left in kilobases. D: genomic sequences around the breakpoints of the dfk deletion. A 2,040-bp sequence containing the Kcnq1 exon 7 was deleted in the WTC-dfk genome. E: molecular diagnosis of the dfk deletion. With use of the primers rKcnq1–51 and rKcnq1–42, a 2,735-bp PCR product was obtained from the WTC genome, while a 695-bp fragment was obtained from the WTC-dfk genome.

auditory organ function, we measured ABR in WTC-*dfk* and WTC rats. In WTC rats, ABR composed of I, II, III, IV, and V peaks was observed with intensity of over 100 dB (Fig. 1*B*). The WTC rats showed an average hearing threshold of 68.3 ± 2.58 dB, whereas all WTC-*dfk* rats exhibited no ABR up to the maximum level (>135 dB) of acoustic stimulation (Fig. 1*B*), indicating that WTC-*dfk* rats were completely deaf.

Identification of the dfk mutation. The pooled SSLP analysis showed a linkage relationship between *D1Rat429* and the *dfk* locus. A genetic linkage study of 240 WTC-*dfk* rats using 19 additional markers on Chr 1 narrowed down *dfk* to a 0.8-cM interval between *D1Kyo9* and *D1Mgh10* (Fig. 2, *A* and *B*). The *dfk* gene showed no recombination with *D1Wox9* in 480 informative meioses. Within the *dfk* locus, four genes, *Cd81* (CD 81 antigen), *Kcnq1* (potassium voltage-gated channel, subfamily Q, member 1), *Mrgrg* (Mas-related G-protein coupled receptor member G), and *Dhcr7* (7-dehydrocholesterol reductase), have been mapped, and these genes were thought to be candidates for *dfk*.

Because human *KCNQ1* mutation is associated with deafness (22), and *Kcnq1*-deficient mice showed similar behavioral

phenotypes to those of WTC-*dfk* rats (5), *Kcnq1* was considered to be the strongest candidate. Northern blot analyses showed that *Kcnq1* transcript of the WTC-dfk was smaller than that of WTC (Fig. 2*C*). Sequencing analyses of the entire coding region and all of the exon-intron boundaries of *Kcnq1* revealed that the entire exon 7 and its flanking sequences were lacking in the WTC-*dfk* rats. The deletion was 2,040 bp in length and flanked with TG dinucleotide tandem repeats (Fig. 2*D*). No nucleotide alternations were observed in the coding sequences of either the *Cd81*, *Mrgrg*, or *Dhcr7* genes between WTC and WTC-*dfk* rats.

To verify and diagnose the deletion at the molecular level, we designed the PCR primers rKcnq1-51 (5′-ACCTGTCAT-GGCTCCCTAGA-3′) and rKcnq1-42 (5′-AGGCTGTCCT-CAGCAAGAAG-3′), which are located outside of the 5′- and 3′-breakpoints, respectively (Fig. 2*B*). These primers yielded a 695-bp PCR product from WTC-*dfk* and a 2,735-bp PCR product from the wild-type WTC (Fig. 2*E*).

Histopathology of the inner ear. To identify the histopathological alterations responsible for the deafness and imbalance observed in WTC-*dfk* rats, we examined the inner ear struc-
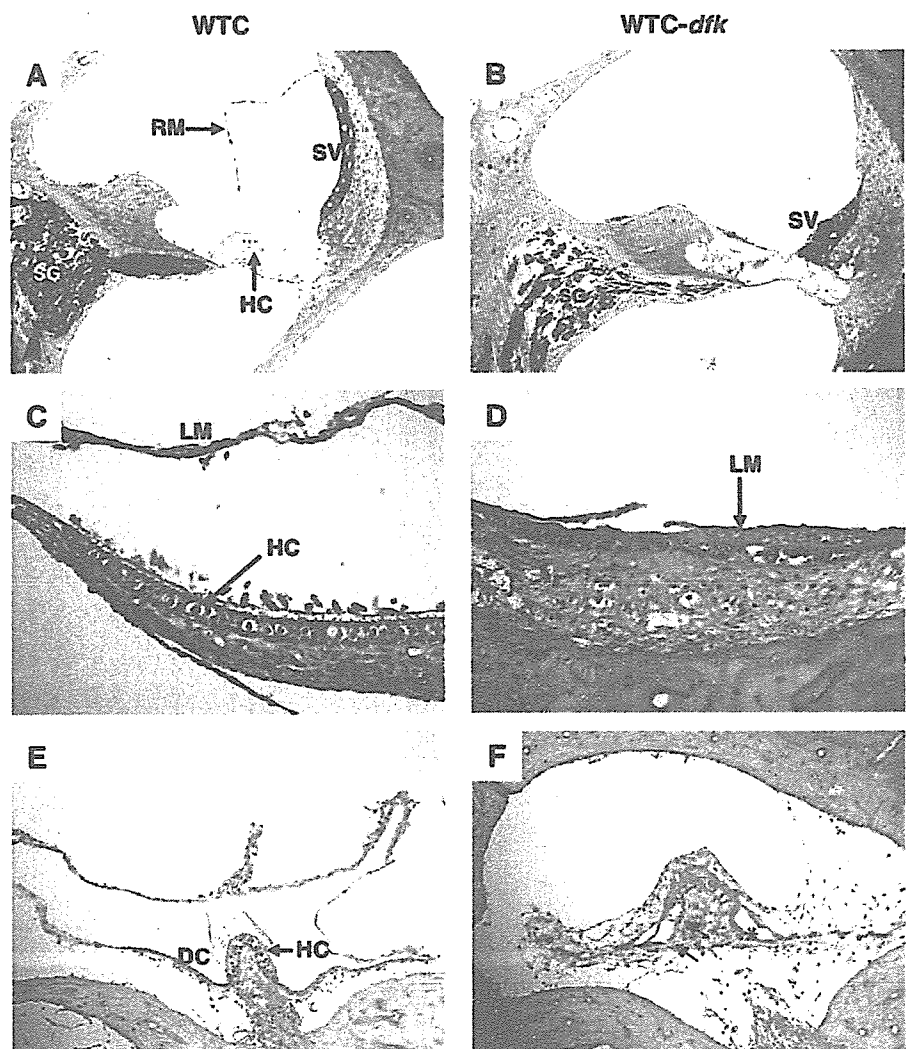

Fig. 3. Histological features of the inner ear of WTC and WTC-*dfk* rats. *A* and *B*: epon-embedded sections of the cochlea stained with toluidine blue. Note that collapsed Reissner's membrane, atrophied stria vascularis, loss of hair cells, and marked reduction of neurons in the spiral ganglion are observed in the 34-wk-old WTC-*dfk* rat. *C* and *D*: details of the saccule macula. Note that the membranous labyrinth is collapsed onto the macula and compresses the statoconia, statoconial membrane, and hair cells in the 34-wk-old WTC-*dfk* rat. *E* and *F*: details of the ampullary crest. Note that the membranous labyrinth is collapsed onto the culpa. A small cavity is present between the membrane and the culpa (indicated by an asterisk), and vacuoles are seen in the marginal region of the ampullary crest (indicated by arrows) in the 34-wk-old WTC-*dfk* rats. DC, dark cell; HC, hair cell; LM, membranous labyrinth; RM, Reissner's membrane; SG, spiral ganglion; SV, stria vascularis.

Table 1. *Comparison of ECG parameters in WTC and WTC-dfk rats*

Parameter	WTC	WTC-*dfk*
HR, bpm	319.4 ± 30.9	350.4 ± 31.1
RR, ms	189.0 ± 16.9	174.2 ± 17.7
PQ, ms	42.3 ± 2.8	40.8 ± 3.6
QRS, ms	15.8 ± 1.9	15.9 ± 2.5
QT, ms	63.7 ± 13.7	86.8 ± 13.7*
QTc, ms	46.4 ± 10.1	65.8 ± 9.2†

All data are presented as means ± SD. Data sets were obtained from adult (12–18 wk) WTC ($n = 6$) and WTC-*dfk* ($n = 6$) rats and were compiled using Student's *t*-test. HR, heart rate; bpm, beats/min; QTc, rate-corrected QT values. *$P < 0.05$ vs. WTC. †$P < 0.01$ vs. WTC.

Table 2. *Acidity of stomach contents in WTC and WTC-dfk rats*

Parameter	WTC	WTC-*dfk*
Gastric volume, ml	2.8 ± 0.9	2.5 ± 0.7
pH	1.47 ± 0.1	7.24 ± 0.2†
Acidity, meq/l	84.2 ± 18.6	ND

All data are presented as means ± SD. Data sets were obtained from WTC ($n = 5$) and WTC-*dfk* ($n = 5$) rats at 11 wk of age and were compiled using Student's *t*-test. ND, not detected. †$P < 0.01$ vs. WTC.

tures. In the cochlea of the 34-wk-old WTC-*dfk* rats, the Reissner's membrane was collapsed and the volume of the cochlear duct was markedly reduced. The stria vascularis was severely atrophied. The inner and outer hair cells in the Corti were degenerated, and swelling of supporting cells was observed. The number of neurons in the spiral ganglion was markedly reduced (Fig. 3*B*). In the macula statica of the utricle, the membranous labyrinth was collapsed onto the macula. The statoconia, the statoconial membrane, and the hair cells were compressed by the collapsed membranous labyrinth, and the endolymphatic space was not observed. The hair cells and supporting cells were severely disarrayed (Fig. 3*D*). In the ampullary crest of the semicircular ducts, the membranous labyrinth was also collapsed and the endolymphatic space was dramatically reduced. The collapsed membranous labyrinth compressed the sensory hair cells and the KCNQ1-expressing dark cells. Vacuoles were observed in the hair cells located in the marginal region of the ampullary crest (Fig. 3*F*).

Prolonged QTc interval in WTC-dfk rats. To evaluate *Kcnq1* function in the rat heart, we examined the ECGs in WTC and WTC-*dfk* rats. Twenty consecutive beats were measured in individual resting animals to obtain the mean values, because ECGs in conscious animals were likely to be contaminated by muscle artifact and noise. The QT interval was measured from

the beginning of the QRS complex to the end of T wave, defined as the point where the T wave merges with the isoelectric line, as described previously (5). The WTC-*dfk* rats demonstrated significant increases in QT and QTc intervals, although there were no significant differences in other parameters such as HR, RR, PQ, and QRS (Table 1). The most striking change in WTC-*dfk* rats occurred in the form of the T wave (Fig. 4). The peak of the T wave was prolonged, and the T-wave area was increased compared with that of WTC rats.

Gastric abnormalities in WTC-dfk rats. To evaluate *Kcnq1* function in the rat stomach, we examined gastric functions of the WTC-*dfk* rats. The volume of the secretion products in the pylorus-ligated stomach collected during the 4-h experimental period was not different between WTC-*dfk* and WTC rats. However, the pH of the stomach fluids was elevated to almost neutral (pH = 7.24 ± 0.2) in the WTC-*dfk* rats, whereas the WTC stomach retained strong acidity (pH = 1.47 ± 0.1). The acidity of the stomach contents could not be detected in the WTC-*dfk* rats, while the acidity of the WTC stomach was 84.2 ± 18.6 meq/l (Table 2). These findings indicated that acid production was impaired in the WTC-*dfk* rats.

The most prominent pathological feature in the stomach of 34-wk-old WTC-*dfk* rats was the appearance of hypertrophic gastric glands in the mucosa of the stomach body (Fig. 5, *B* and *C*). Such lesions were scattered in the mucosa, and their cytoplasm was deeply stained with eosin. Additionally, dilatation of the fundic glands and fibrosis in the lamina propria were observed in the stomach body of WTC-*dfk* rats. Fibrosis was

WTC

PQ QRS

QT

| 0 | 100 | 200 | 300 |

(ms)

WTC-*dfk*
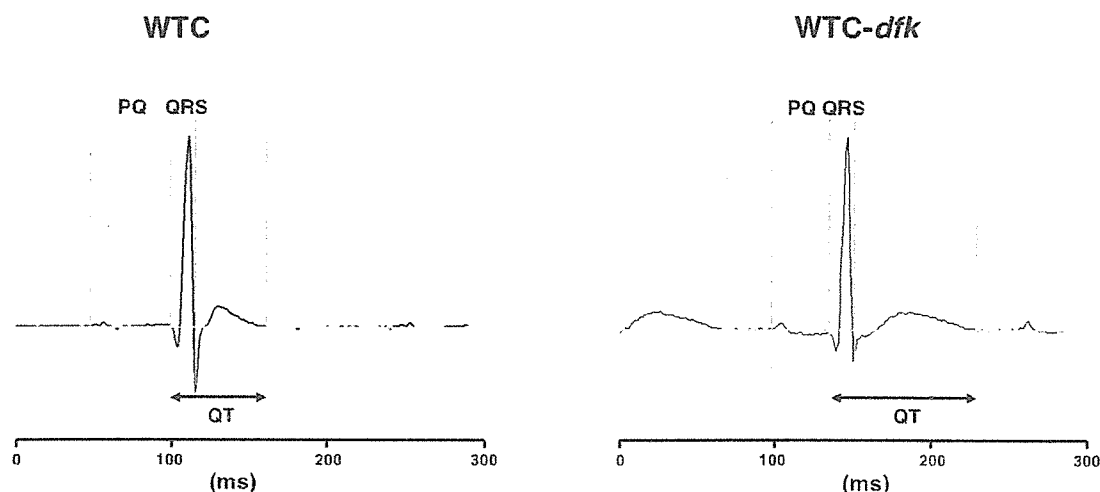
PQ QRS

QT

| 0 | 100 | 200 | 300 |

(ms)

Fig. 4. Representative surface electrocardiogram (ECG) trace recorded in vivo in WTC and WTC-*dfk* rats. Representative ECG traces obtained from adult (12–18 wk) WTC ($n = 6$) and WTC-dfk ($n = 6$) rats. Each parameter (PQ, QRS, QT) is indicated. Note that the QT interval was prolonged in WTC-*dfk* compared with the wild-type coisogenic control WTC rat. Depicted tracings were selected as representative of the particular phenotype.
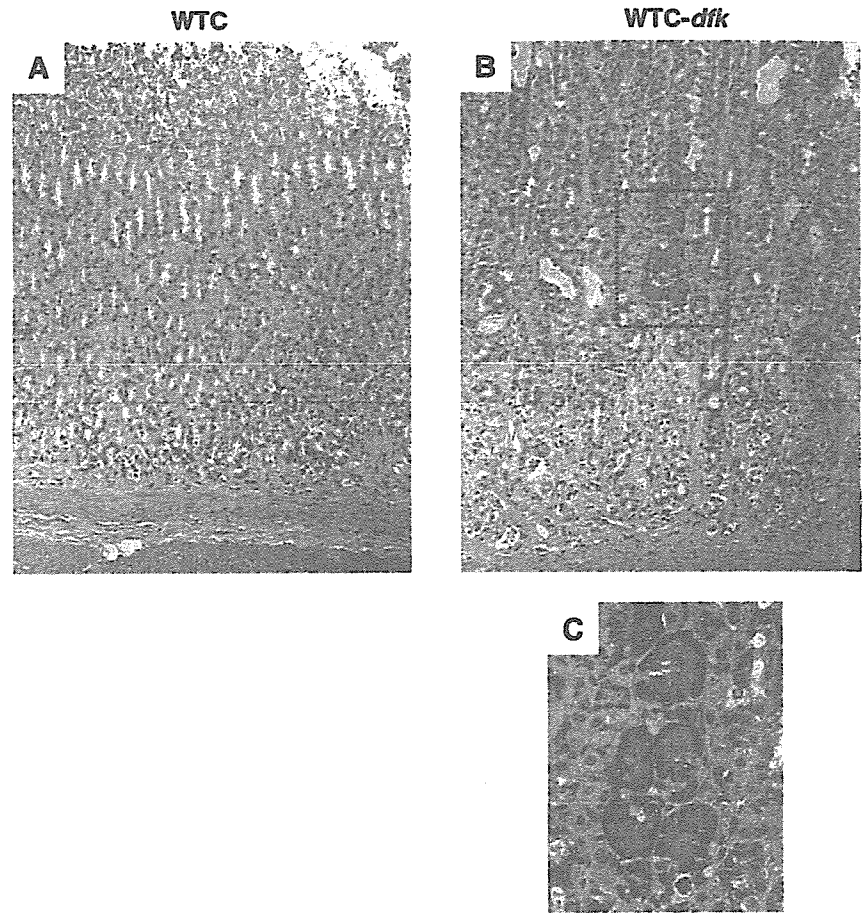
WTC

WTC-*dfk*

Fig. 5. Histopathological features of the stomach of WTC and WTC-*dfk* rats. Mucosa of the stomach body of a 34-wk-old WTC rat (*A*) and WTC-*dfk* rat (*B*). Note that hypertrophic eosinophilic cells, scattered in the mucosa, are found in the WTC-*dfk* rat. Fibrosis was distributed in the lamina propria, especially in the bottom part of the mucosa. *C*: Higher magnification of the hypertrophic eosinophilic cells.

prominent at the bottom part of the mucosa (Fig. 5*B*). No pathological alteration was observed in the pylorus of the WTC-*dfk* rats.

Hypertension in WTC-dfk rats. To examine the physiological phenotypic characteristics of the WTC-*dfk* rats, we collected phenotypic data about blood pressure, biochemical blood test values, hematology, and urology. The most striking finding was hypertension in the WTC-*dfk* rats. They showed significant increases in the systolic blood pressure (SBP) compared with WTC (165.8 ± 22 vs. 125.8 ± 14.4 mmHg, $P =$ 0.0001). The blood pressure level of WTC-*dfk* rats was highly placed on the ranking list of the SBP of 98 rat inbred strains of the Rat Phenome Project of the NBRP in Japan (**http:// www.anim.med.kyoto-u.ac.jp/nbr**) (18). The SBP of WTC-*dfk* rats was greater than the mean value plus one standard deviation of the SBP of the 98 rat strains (142.7 ± 19.4 mmHg), while that of WTC rats was within the mean value plus one standard deviation.

DISCUSSION

We have described here the molecular basis and phenotypes of a novel mutation of the rat *Kcnq1* gene. WTC-*dfk* rats had an intragenic deletion that included whole exon 7 of the *Kcnq1* gene. The rat *Kcnq1* cDNA encodes a 669-amino acid polypeptide with six membrane-spanning segments and a pore-associated domain (13). *Kcnq1* exon 7 is 111 bp in length and

encodes a 37-amino acid peptide that forms a pore-associated domain and part of the sixth transmembrane domain. Therefore, the *dfk* deletion allele was thought to result in a smaller protein that lacked the pore, which plays important roles in generating K^+ current.

We found several intriguing phenotypes of the WTC-*dfk* rat. First, these rats showed circular movements, imbalance, and complete deafness. Histological analyses demonstrated the marked reduction of the endolymph of the inner ear and the collapse of sensory hair cells. These findings implied that endolymph reduction followed by hair cell collapses resulted in inner ear defects in the WTC-*dfk* rats. *Kcnq1*-deficient mice also show circular movements, imbalance, deafness, and inner ear pathologies that are very similar to those observed in the WTC-*dfk* rats (5, 16). The phenotypic similarities and deduced functions of the mutated KCNQ1 of the WTC-*dfk* rat suggested that WTC-*dfk* rats would be deficient for KCNQ1 protein.

Second, the WTC-*dfk* rats manifested prolonged QT interval and abnormal T-wave form in the ECG, indicating that the ventricular repolarization was prolonged in the WTC-*dfk* rats. The ventricular repolarization derives from transient outward K^+ currents (I_{to}) and delayed, outwardly rectifying K^+ currents (I_K) (21). In the rat myocytes, two transient outward K^+ currents, $I_{to,f}$ and $I_{to,s}$ (1, 36), and five distinct delayed rectifier currents, I_{Kr}, I_{Kur}, I_K, $I_{K,slow}$, and I_{ss}, have been identified (1, 3, 20). However, I_{Ks} current generated from KCNQ1/KCNE1

complex is not a prominent repolarizing current in adult rats or in mice. Therefore, the cardiac phenotype seen in the WTC-*dfk* rats would not be a direct effect of KCNQ1 deficiency but would be induced by extacardiac stimuli such as autonomic nerve and hormonal factors (32, 35). This idea is supported by the data on the cardiac phenotypes of the *Kcnq1*-deficient mice. They displayed abnormal T-wave form and prolongation of the QT interval when measured in vivo, but not in isolated hearts (5). In addition, nicotine challenge of the isolated heart and acute stress due to saline injection in vivo revealed that sympathetic stimulation induced a long-QT phenotype in *Kcnq1*-deficient mice (28).

Third, we found achlorhydria in the WTC-*dfk* rats. Because gastric H$^+$ is secreted by the H$^+$/K$^+$-ATPase with coupling to the uptake of the luminal K$^+$ (23, 37), it is possible that the mutated KCNQ1 polypeptide fails to transport K$^+$ into the gastric lumen. Histological findings of the WTC-*dfk* stomach were hypertrophy of the gastric glands and fibrosis in the lamina propria. Because the administration of proton pump inhibitor sometimes induces hypertrophic gastric glands in the rat, these pathological changes are thought to have been produced as a direct effect of the elevation of pH in the stomach (4). *Kcnq1*-deficient mice also show achlorhydria and increased weight of the stomach resulting from mucous neck cell hyperplasia (8, 16).

It is likely that the lower body weight found in the WTC-*dfk* rats is related to their hyperactivity associated with the inner ear defects. Additionally, the loss of *Kcnq1* functions in the stomach, the intestine, or the pancreas might give another possible explanation. Gastric H$^+$ is required to converse pepsinogen to pepsin, the protease largely responsible for initiating the digestion of proteins in the stomach. KCNQ1 expressed in the epithelium of the small intestine and colon is believed to regulate K$^+$ transport into the lumen (25). Luminal K$^+$ is required for transepithelial Cl$^-$ secretion, which regulates the osmolality of the intestinal or colonic mucus. In the insulin-secreting cells, the KCNQ1 channels might play a role in regulation of the insulin secretion (29). Thus investigating the digestive capability and insulin secretion levels in the WTC-*dfk* rats would be helpful for determining the cause of the lower body weight.

Lastly, the WTC-*dfk* rats displayed hypertension. This is the first evidence that *Kcnq1* might be involved in the regulation of blood pressure in the rat. Hypertension is provoked by a variety of etiologies. We have not yet determined which factor(s) induces hypertension in the WTC-*dfk* rats, but it seems likely that it is due to a defect in reabsorption in the proximal tubule of the kidney. In the mouse kidney, KCNQ1 colocalizes with KCNE1 in the brush border of the mid to late proximal convoluted tubule as well as in the proximal straight tubule (30). It is thought that the KCNQ1/KCNE1 complex would make K$^+$ flux to the lumen, which is essential to counteract membrane depolarization due to electrogenic Na$^+$-coupled transport (30). Considering the important role of reabsorption in the regulation of blood pressure, it is possible that there might be some defect(s) in the kidney proximal tubule of the WTC-*dfk* rats.

WTC-*dfk* rats offer a sophisticated genetic system for studies of the physiological functions of KCNQ1, because this strain has a strict control strain, WTC. The two strains are coisogenic and have an identical genetic background except for the *dfk*

deletion. Thus phenotypic differences found between them would only result from the *dfk* mutation, which would imply the involvement of the *Kcnq1* in such phenotypes. This genetic system was obtained simply by a spontaneous mutation arising in an inbred strain. In the gene knockout mouse, one cannot exclude effects of genes closely linked to the targeted gene on their phenotypes, even after producing congenic strains (26). *Kcnq1* has been shown to be associated with several diseases such as long QT, deafness, achlorhydria, and hypertension. To develop more effective treatments for these disorders, WTC-*dfk* could offer a powerful new tool as a *Kcnq1*-related disease model. Furthermore, because KCNQ1 is expressed in various epithelial tissues, including lung, colon, small intestine, and thymus (7, 33), the functions of KCNQ1 in these tissues could be clarified using the coisogenic system of WTC-*dfk* and WTC.

ACKNOWLEDGMENTS

GRANTS

REFERENCES

1. **Apkon M and Nerbonne JM.** Characterization of two distinct depolarization-activated K$^+$ currents in isolated adult rat ventricular myocytes. *J Gen Physiol* 97: 973–1011, 1991.

2. **Barhanin J, Lesage F, Guillemare E, Fink M, Lazdunski M, and Romey G.** K(V)LQT1 and IsK (minK) proteins associate to form the I(Ks) cardiac potassium current. *Nature* 384: 78–80, 1996.

3. **Boyle WA and Nerbonne JM.** Two functionally distinct 4-aminopyridine-sensitive outward K$^+$ currents in rat atrial myocytes. *J Gen Physiol* 100: 1041–1067, 1992.

4. **Carlsson E, Larsson H, Mattsson H, Ryberg B, and Sundell G.** Pharmacology and toxicology of omeprazole—with special reference to the effects on the gastric mucosa. *Scand J Gastroenterol Suppl* 118: 31–38, 1986.

5. **Casimiro MC, Knollmann BC, Ebert SN, Vary JC Jr, Greene AE, Franz MR, Grinberg A, Huang SP, and Pfeifer K.** Targeted disruption of the *Kcnq1* gene produces a mouse model of Jervell and Lange-Nielsen Syndrome. *Proc Natl Acad Sci USA* 98: 2526–2531, 2001.

6. **Dedek K and Waldegger S.** Colocalization of KCNQ1/KCNE channel subunits in the mouse gastrointestinal tract. *Pflügers Arch* 442: 896–902, 2001.

7. **Demolombe S, Franco D, de Boer P, Kuperschmidt S, Roden D, Pereon Y, Jarry A, Moorman AF, and Escande D.** Differential expression of KvLQT1 and its regulator IsK in mouse epithelia. *Am J Physiol Cell Physiol* 280: C359–C372, 2001.

8. **Elso CM, Lu X, Culiat CT, Rutledge JC, Cacheiro NL, Generoso WM, and Stubbs LJ.** Heightened susceptibility to chronic gastritis, hyperplasia and metaplasia in *Kcnq1* mutant mice. *Hum Mol Genet* 13: 2813–2821, 2004.

9. **Grahammer F, Herling AW, Lang HJ, Schmitt-Graff A, Wittekindt OH, Nitschke R, Bleich M, Barhanin J, and Warth R.** The cardiac K$^+$ channel KCNQ1 is essential for gastric acid secretion. *Gastroenterology* 120: 1363–1371, 2001.

10. **Grahammer F, Warth R, Barhanin J, Bleich M, and Hug MJ.** The small conductance K$^+$ channel, KCNQ1: expression, function, and subunit composition in murine trachea. *J Biol Chem* 276: 42268–42275, 2001.

11. **Heitzmann D, Grahammer F, von Hahn T, Schmitt-Graff A, Romeo E, Nitschke R, Gerlach U, Lang HJ, Verrey F, Barhanin J, and Warth**

R. Heteromeric KCNE2/KCNQ1 potassium channels in the luminal membrane of gastric parietal cells. *J Physiol* 561: 547–557, 2004.

12. Jervell A and Lange-Nielsen F. Congenital deaf-mutism, functional heart disease with prolongation of the Q-T interval and sudden death. *Am Heart J* 54: 59–68, 1957.

13. Kunzelmann K, Hubner M, Schreiber R, Levy-Holzman R, Garty H, Bleich M, Warth R, Slavik M, von Hahn T, and Greger R. Cloning and function of the rat colonic epithelial K⁺ channel KVLQT1. *J Membr Biol* 179: 155–164, 2001.

14. Kuramoto T, Kitada K, Inui T, Sasaki Y, Ito K, Hase T, Kawagachi S, Ogawa Y, Nakao K, Barsh GS, Nagao M, Ushijima T, and Serikawa T. *Attractin/mahogany/zitter* plays a critical role in myelination of the central nervous system. *Proc Natl Acad Sci USA* 98: 559–564, 2001.

15. Kuramoto T, Yamasaki K, Kondo A, Nakajima K, Yamada M, and Serikawa T. Production of WTC.ZI-*zi* rat congenic strain and its pathological and genetic analyses. *Exp Anim* 47: 75–81, 1998.

16. Lee MP, Ravenel JD, Hu RJ, Lustig LR, Tomaselli G, Berger RD, Brandenburg SA, Litzi TJ, Bunton TE, Limb C, Francis H, Gorelikow M, Gu H, Washington K, Argani P, Goldenring JR, Coffey RJ, and Feinberg AP. Targeted disruption of the *Kvlqt1* gene causes deafness and gastric hyperplasia in mice. *J Clin Invest* 106: 1447–1455, 2000.

17. Mall M, Wissner A, Schreiber R, Kuehr J, Seydewitz HH, Brandis M, Greger R, and Kunzelmann K. Role of K(V)LQT1 in cyclic adenosine monophosphate-mediated Cl⁻ secretion in human airway epithelia. *Am J Respir Cell Mol Biol* 23: 283–289, 2000.

18. Mashimo T, Voigt B, Kuramoto T, and Serikawa T. Rat Phenome Project: the untapped potential of existing rat strains. *J Appl Physiol* 98: 371–379, 2005.

19. Mitchell GF, Jeron A, and Koren G. Measurement of heart rate and Q-T interval in the conscious mouse. *Am J Physiol Heart Circ Physiol* 274: H747–H751, 1998.

20. Nerbonne JM. Molecular basis of functional voltage-gated K⁺ channel diversity in the mammalian myocardium. *J Physiol* 525: 285–298, 2000.

21. Nerbonne JM and Kass RS. Physiology and molecular biology of ion channels contributing to ventricular repolarization. In: *Cardiac Repolarization. Bridging Basic and Clinical Science*, edited by Gussal IB and Antzelevitch C. Totowa, NJ: Humana, 2003, p. 25–62.

22. Neyroud N, Tesson F, Denjoy I, Leibovici M, Donger C, Barhanin J, Faure S, Gary F, Coumel P, Petit C, Schwartz K, and Guicheney P. A novel mutation in the potassium channel gene KVLQT1 causes the Jervell and Lange-Nielsen cardioauditory syndrome. *Nat Genet* 15: 186–189, 1997.

23. Reenstra WW and Forte JG. Characterization of K⁺ and Cl⁻ conductances in apical membrane vesicles from stimulated rabbit oxyntic cells. *Am J Physiol Gastrointest Liver Physiol* 259: G850–G858, 1990.

24. Sanguinetti MC, Curran ME, Zou A, Shen J, Spector PS, Atkinson DL, and Keating MT. Coassembly of K(V)LQT1 and minK (IsK)

proteins to form cardiac I(Ks) potassium channel. *Nature* 384: 80–83, 1996.

25. Schroeder BC, Waldegger S, Fehr S, Bleich M, Warth R, Greger R, and Jentsch TJ. A constitutively open potassium channel formed by KCNQ1 and KCNE3. *Nature* 403: 196–199, 2000.

26. Silver LM. *Mouse Genetics.* New York: Oxford Univ. Press, 1995.

27. Taylor BA, Navin A, and Phillips SJ. PCR-amplification of simple sequence repeat variants from pooled DNA samples for rapidly mapping new mutations of the mouse. *Genomics* 21: 626–632, 1994.

28. Tosaka T, Casimiro MC, Rong Q, Tella S, Oh M, Katchman AN, Pezzullo JC, Pfeifer K, and Ebert SN. Nicotine induces a long QT phenotype in *Kcnq1*-deficient mouse hearts. *J Pharmacol Exp Ther* 306: 980–987, 2003.

29. Ullrich S, Su J, Ranta F, Wittekindt OH, Ris F, Rosler M, Gerlach U, Heitzmann D, Warth R, and Lang F. Effects of I(Ks) channel inhibitors in insulin-secreting INS-1 cells. *Pflügers Arch* 451: 428–436, 2005.

30. Vallon V, Grahammer F, Richter K, Bleich M, Lang F, Barhanin J, Volkl H, and Warth R. Role of KCNE1-dependent K⁺ fluxes in mouse proximal tubule. *J Am Soc Nephrol* 12: 2003–2011, 2001.

31. Vetter DE, Mann JR, Wangemann P, Liu J, McLaughlin KJ, Lesage F, Marcus DC, Lazdunski M, Heinemann SF, and Barhanin J. Inner ear defects induced by null mutation of the isk gene. *Neuron* 17: 1251–1264, 1996.

32. Walsh KB and Kass RS. Regulation of a heart potassium channel by protein kinase A and C. *Science* 242: 67–69, 1988.

33. Wang Q, Curran ME, Splawski I, Burn TC, Millholland JM, Van-Raay TJ, Shen J, Timothy KW, Vincent GM, de Jager T, Schwartz PJ, Toubin JA, Moss AJ, Atkinson DL, Landes GM, Connors TD, and Keating MT. Positional cloning of a novel potassium channel gene: KVLQT1 mutations cause cardiac arrhythmias. *Nat Genet* 12: 17–23, 1996.

34. Ward OC. A new familial cardiac syndrome in children. *J Ir Med Assoc* 54: 103–106, 1964.

35. Washizuka T, Horie M, Watanuki M, and Sasayama S. Endothelin-1 inhibits the slow component of cardiac delayed rectifier K⁺ currents via a pertussis toxin-sensitive mechanism. *Circ Res* 81: 211–218, 1997.

36. Wickenden AD, Jegla TJ, Kaprielian R, and Backx PH. Regional contributions of Kv1.4, Kv4.2, and Kv4.3 to transient outward K⁺ current in rat ventricle. *Am J Physiol Heart Circ Physiol* 276: H1599–H1607, 1999.

37. Wolosin JM and Forte JG. Stimulation of oxyntic cell triggers K⁺ and Cl⁻ conductances in apical H⁺-K⁺-ATPase membrane. *Am J Physiol Cell Physiol* 246: C537–C545, 1984.

38. Yang WP, Levesque PC, Little WA, Conder ML, Shalaby FY, and Blanar MA. KvLQT1, a voltage-gated potassium channel responsible for human cardiac arrhythmias. *Proc Natl Acad Sci USA* 94: 4017–4021, 1997.

MUTATION IN BRIEF

Genotype-Phenotype Correlations of *KCNJ2* Mutations in Japanese Patients With Andersen-Tawil Syndrome

Yoshisumi Haruna[1†], Atsushi Kobori[1†], Takeru Makiyama[1], Hidetada Yoshida[1], Masaharu Akao[1], Takahiro Doi[1], Keiko Tsuji[2], Seiko Ono[1], Yukiko Nishio[1], Wataru Shimizu[3], Takehiko Inoue[4], Tomoaki Murakami[5], Naoya Tsuboi[6], Hideo Yamanouchi[7], Hiroya Ushinohama[8], Yoshihide Nakamura[9], Masao Yoshinaga[10], Hitoshi Horigome[11], Yoshifusa Aizawa[12], Toru Kita[1], and Minoru Horie[2*]

[1]*Department of Cardiovascular Medicine, Kyoto University Graduate School of Medicine, Kyoto, Japan;* [2]*Department of Cardiovascular and Respiratory Medicine, Shiga University of Medical Science, Otsu, Japan;* [3]*Division of Cardiology, Department of Internal Medicine, National Cardiovascular Center, Suita, Japan;* [4]*Division of Child Neurology, Institute of Neurological Sciences, Faculty of Medicine, Tottori University, Yonago, Japan;* [5]*Department of Pediatrics, Hokkaido University Graduate School of Medicine, Sapporo, Japan;* [6]*Department of Cardiology, Nagoya Daini Red Cross Hospital, Nagoya, Japan;* [7]*Department of Pediatrics, Dokkyo University School of Medicine, Tochigi, Japan;* [8]*Pediatric Cardiology Division, Fukuoka Children's Hospital and Medical Center for Infectious Diseases, Fukuoka, Japan;* [9]*Department of Pediatric Cardiology, Japanese Red Cross Society Wakayama Medical Center, Wakayama, Japan;* [10]*National Hospital Organization Kyushu Cardiovascular Center, Kagoshima, Japan;* [11]*Department of Pediatrics, Institute of Clinical Medicine, University of Tsukuba, Tsukuba, Japan;* [12]*Department of Cardiology, Niigata University Graduate School of Medical and Dental Sciences, Niigata, Japan*

[†]*These authors equally contributed to this work.*

*Correspondence to: Minoru Horie, MD, PhD, Department of Cardiovascular and Respiratory Medicine, Shiga University of Medical Science, Seta Tsukinowa-cho, Otsu, Shiga 520-2192, Japan; Tel.: +81-77-548-2213; Fax: +81-77-543-5839; E-mail: horie@belle.shiga-med.ac.jp

Communicated by Johannes Zschocke

Andersen-Tawil syndrome (ATS) is a rare inherited disorder characterized by periodic paralysis, mild dysmorphic features, and QT or QU prolongation with ventricular arrhythmias in electrocardiograms (ECGs). Mutations of *KCNJ2*, encoding the human inward rectifying potassium channel Kir 2.1, have been identified in patients with ATS. We aimed to clarify the genotype-phenotype correlations in ATS patients. We screened 23

clinically diagnosed ATS patients from 13 unrelated Japanese families. Ten different forms of *KCNJ2* mutations were identified in the 23 ATS patients included in this study. Their ECGs showed normal QTc intervals and abnormal U waves with QUc prolongation and a variety of ventricular arrhythmias. Especially, bidirectional ventricular tachycardia (VT) was observed in 13 of 23 patients (57%). Periodic paralysis was seen in 13 of 23 carriers (57%), dysmorphic features in 17 (74%), and seizures during infancy in 4 (17%). Functional assays for the two novel *KCNJ2* mutations (c. 200G>A (p. R67Q) and c. 436G>A (p. G146S)) displayed no functional inward rectifying currents in a heterologous expression system and showed strong dominant negative effects when co-expressed with wild-type *KCNJ2* channels (91% and 84% reduction at −50 mV respectively compared to wild-type alone). Immunocytochemistry and confocal imaging revealed normal trafficking for mutant channels. In our study, all of the clinically diagnosed ATS patients had *KCNJ2* mutations and showed a high penetrance with regard to the typical cardiac phenotypes: predominant U wave and ventricular arrhythmias, typically bidirectional VT. © 2007 Wiley-Liss, Inc.

INTRODUCTION

Andersen-Tawil syndrome (ATS, MIM# 170390) is a rare autosomal dominant disorder characterized by classical triad: (1) ventricular tachyarrhythmias associated with QT prolongation in electrocardiograms (ECGs), (2) periodic paralysis, and (3) dysmorphic features (Andersen, et al., 1971; Canun, et al., 1999; Sansone, et al., 1997; Tawil, et al., 1994). Plaster et al. revealed that mutations in *KCNJ2* (MIM# 600681) caused the syndrome in the majority of clinically diagnosed ATS families (Plaster, et al., 2001). *KCNJ2* encodes a pore-forming subunit of inwardly rectifying potassium channels (Kir 2.1), a critical contributor for the I_{K1} current, which maintains normal resting membrane potentials and regulates the final phase of action potential repolarization in various types of cells (Kubo, et al., 1993; Raab-Graham, et al., 1994). To date, more than 30 *KCNJ2* mutations were identified and reported to be responsible for ATS (Ai, et al., 2002; Bendahhou, et al., 2005; Davies, et al., 2005; Donaldson, et al., 2003; Hosaka, et al., 2003; Plaster, et al., 2001; Tristani-Firouzi, et al., 2002; Zhang, et al., 2005). Most mutations in *KCNJ2* showed loss-of-function and dominant negative suppression effects (Tristani-Firouzi, et al., 2002), and a mutation, p.S136F, has been shown to suppress the native I_{K1} in neonatal rat cardiomyocytes (Lange, et al., 2003).

In contrast to the relatively homogenous change in functional outcome as a result of the mutations, ATS patients displayed a wide range of penetrance and severity of clinical phenotypes (Plaster, et al., 2001). This perplexity makes it difficult for physicians to properly diagnose the syndrome. Indeed, some cases have been diagnosed and treated as long QT syndrome (LQTS) and others as periodic paralysis. Tristani-Firouzi et al. performed extensive genetic and phenotypic analyses of ATS patients from 17 families and suggested that ATS might be classified as a new subtype of LQTS (referred to as *KCNJ2*-associated LQTS (LQT7)) (Tristani-Firouzi, et al., 2002). Recently, Zhang et al. reviewed the ECGs of 96 ATS patients with *KCNJ2* mutations and revealed the median QTc interval in ATS patients to be within the normal range (Zhang, et al., 2005). They concluded that *KCNJ2*-associated ATS is not a subtype of LQTS and recommended to have them annotated as ATS1. In a study on guinea pig hearts transfected with a dominant negative *KCNJ2* mutant, Miake et al. demonstrated that suppression of I_{K1} decelerated the action potential repolarization, prolonged the action potential duration, and depolarized the resting membrane potential. They also observed that the suppression of I_{K1} caused QTc prolongation on surface ECGs.

In order to clarify the genotype-phenotype correlations in Japanese ATS patients, we carried out a complete screening of *KCNJ2* in 23 ATS patients and investigated their clinical manifestations.

METHODS

Study Subjects

Twenty-three clinically diagnosed Japanese ATS patients (from 13 unrelated families) were enrolled in this study from 12 institutes in Japan. Individuals were diagnosed as being affected with ATS if 2 or 3 of the following criteria were present: (1) episodes of muscle weakness, (2) cardiac involvement, and/or (3) dysmorphology as previously described (Donaldson, et al., 2003; Tristani-Firouzi, et al., 2002). The presence of periodic paralysis was based on standard criteria (McManis, et al., 1986). Cardiac involvement was determined by the presence of ventricular arrhythmias (frequent premature ventricular contractions (PVCs), bigeminy, ventricular tachycardia (VT)), prolongation of the corrected QT interval (QTc) and/or a prominent U wave. Subjects were classified as having QT prolongation if the QTc exceeded 440 milliseconds (ms) for males and 460 ms for females, in accordance with standard criteria (Keating, et al., 1991). The QT interval was defined from the onset of QRS to the end of the T wave. The U wave was defined as an early diastolic deflection after the end of the T wave. The QU interval was defined from the onset of QRS to the end of the U wave. QT and QU intervals were corrected according to Bazzett's formula (Bazzett, 1920; Zhang, et al., 2005). The end of the T or U wave was the point at which a tangent drawn to the steepest portion of the terminal part of the T or U wave crossed the isoelectric line (Yan and Antzelevitch, 1998). Because a prominent U wave is fused to the next PQ segment in some cases, we defined the isoelectric line as a segment connecting two points preceding consecutive QRS complexes. Abnormal U waves were judged by the following criteria: (a) wave amplitude ≥ 0.2 mV (Lepeschkin, 1972) or (b) amplitude larger than preceding T wave (Lepeschkin, 1969).

Dysmorphology was defined by the presence of 2 or more of the following: (a) low-set ears, (b) hypertelorism (wide-set eyes), (c) small mandible, (d) clinodactyly (permanent lateral or medial curve of a finger or toe), and (e) syndactyly (persistent webbing between fingers or toes) (Tristani-Firouzi, et al., 2002).

In order to elucidate the genetic differences between ATS and LQTS, we also screened *KCNJ2* mutations in 74 LQTS probands from 74 unrelated families. They displayed no clinical signs compatible with ATS except for cardiac manifestations.

DNA Isolation and Mutation Analysis

The protocol for genetic analysis was approved by the Institutional Ethics Committee and was performed under its guidelines. All patients provided an informed consent before the genetic analysis was carried out. Genomic DNA was isolated from leukocyte nuclei using a DNA extraction kit, QIAamp DNA Blood midi kit, (QIAGEN GmbH, Hilden, Germany). Genetic screening for *KCNJ2* was performed by polymerase chain reaction/single-strand conformation polymorphism (PCR-SSCP) analysis (Yoshida, et al., 1999) or denaturing high-performance liquid chromatography (DHPLC) using WAVE System Model 3500 (Transgenomic, Omaha, NE, USA) (Ning, et al., 2003). Abnormal conformers were amplified via PCR, and sequencing was performed on an ABI PRISM3100 DNA sequencer (Applied Biosystems, Wellesley, MA, USA). The cDNA sequence numbering was based upon GenBank reference sequence NM_000891.2 for *KCNJ2* and NM_000218.2 for *KCNQ1* (the first adenosine in the initiator ATG was designed as +1).

In Vitro Mutagenesis

With regard to the novel *KCNJ2* mutations, site-directed mutagenesis was employed to construct mutants as described previously (Hosaka, et al., 2003). Briefly, human *KCNJ2* cDNA was subcloned into the pCMS-EGFP plasmid (Clontech, Palo Alto, CA, USA). We engineered *KCNJ2* mutants using a site-directed mutagenesis kit, QuickChange II XL (Stratagene, La Jolla, CA, USA). The presence of mutations was confirmed by sequencing.

Electrophysiological Experiments and Data Analysis

To assess the functional modulation of *KCNJ2* channels, we employed a heterologous expression system with COS7 cells (Kubota, et al., 2000). Briefly, the cells were transiently transfected by the LipofectAMINE method as directed in the manufacture's instructions (Invitrogen, Carlsbad, CA, USA), using a 1.0 µg/35 mm dish of pCMS-EGFP/*KCNJ2* (wild type (WT) and/or mutant). For electrophysiological experiments, GFP-positive cells were selected 24 to 72 hours after transfection. Current measurement was conducted by the conventional whole-cell configuration of patch-clamp techniques at 37°C, using an Axopatch 200A patch clamp amplifier and a Digidata 1322A digitizer (Axon Instruments, Foster City, CA, USA). pClamp software (version 9.0, Axon Instruments)

was used to generate voltage pulse protocols and for data acquisition. Currents were evoked by 150 ms square pulses applied in 10 mV increments to potentials ranging from −140 mV to +30 mV from a holding potential of − 80 mV. Pipettes were filled with a solution containing (in mM): K-aspartate 60, KCl 65, KH_2PO_4 1, $MgCl_2$ 2, EDTA 3, K_2ATP 3 and HEPES 5 adjusted to pH 7.4 using KOH, and had a resistance of 3.0 to 5.0 MΩ. The bath solution contained (in mM): NaCl 140, KCl 5.4, $MgCl_2$ 0.5, $CaCl_2$ 1.8, NaH_2PO_4 0.33, glucose 5.5, and HEPES 5 (pH 7.4 with NaOH) (Yoshida, et al., 1999). All the data are shown as mean ± SEM. Where appropriate, Student's unpaired t-test was used; a value of $P < 0.05$ was considered statistically significant.

Immunocytochemistry
The hemaggulutinin (HA) epitope (YPYDVPDVA) was introduced into the pCMS-EGFP/*KCNJ2* (WT and mutants) between Ala-115 and Ser-116 (extracellular lesion between TM1 and TM2) as previously described (Ballester, et al., 2006). COS7 cells were transfected with 1.0 μg of plasmid DNA in 35 mm glass-bottom dishes. Forty-eight hours later, the cells were washed twice with phosphate buffered saline (PBS), followed by incubation with a mouse anti-HA primary antibody (1:500) (Covance Research Products, Inc., Berkeley, CA, USA) for 30 minutes at 37°C. The cells were then washed twice with PBS and incubated with an anti-mouse antibody conjugated to the Alexa 594 fluorophor (1:500) (Molecular Probes, Eugene, OR, USA) as a secondary antibody for 30 minutes at 37°C. Finally, cells were washed with and immersed in PBS, and confocal imagings were obtained with a Zeiss LSM 510 (Carl Zeiss GmbH, Jena, Germany).

RESULTS

KCNJ2 **Mutation Analysis**
Figure 1 and Table 1 show the mutations and clinical findings of 23 ATS patients (9 males/14 females; mean 23.0 ± 3.1 years old). There were 13 probands from 13 unrelated families. We found 10 different heterozygous *KCNJ2* mutations (two were novel) in the 23 ATS patients examined in this study: c.199C>T (p.R67W) (Andelfinger, et al., 2002); c.200G>A (p.R67Q); c.430G>A (p.G144S) (Kobori, et al., 2004); c.436G>A (p.G146S); c.574A>G (p.T192A) (Ai, et al., 2002); c.644G>A (p.G215D) (Hosaka, et al., 2003); c.652C>T (p.R218W) (Plaster, et al., 2001); c.653G>A (p.R218Q) (Tristani-Firouzi, et al., 2002); c.899G>T (p.G300V) (Tristani-Firouzi, et al., 2002); and c.926C>T (p.T309I) (Bendahhou, et al., 2005). R67Q and G146S were novel mutations. Arginine at codon 67 is implicated in binding membrane-associated phoshatidylinositol 4,5-bisphosphate (PIP_2), and has been reported to be a hot spot for ATS mutations (Donaldson, et al., 2003; Zhang, et al., 2005), but the substitution of arginine with glutamine (R67Q) is a novel mutation. G146S is also a novel mutation located at an essential region known as the K^+ channel signature sequence that serves as a principal ion selective filter (Doyle, et al., 1998). Therefore, both R67Q and G146S are supposed to cause substantial effects to *KCNJ2* channels.

In 8 kindred (K-024, K-037, K-178, K-180, K240, K-323, KJ-01, and KJ-02, Table 1) the mutations were inherited from parents. In contrast, they were *de novo* in 3 probands of 3 kindred (K-179, K-201, and K-324) and were undetermined in 2 kindred (N-01 and KJ-03) because detailed family information was not available. These *KCNJ2* variants were not present in 100 normal controls (200 alleles). Analysis for other known LQTS-responsible genes (*KCNQ1*, *KCNH2*, *SCN5A*, *KCNE1*, and *KCNE2*) revealed that K-024 proband and her son were also heterozygous for a *KCNQ1* mutation (c.1022C>T (p.A341V))(Kobori, et al., 2004).

In 74 LQTS patients, we found one novel *KCNJ2* variant (c.1051C>T (p.P351S)) in a 74-year-old female who had suffered from syncope and received a pacemaker implantation. In addition, genetic analysis had revealed that she was a carrier of c.1927G>A (p.G643S) (*KCNQ1*). This variant (P351S-*KCNJ2*) could not be identified in 100 healthy controls.

The cDNA sequence numbering was based upon GenBank reference sequence NM_000891.2 for *KCNJ2* and NM_000218.2 for *KCNQ1* (the first adenosine in the initiator ATG was designed as +1).
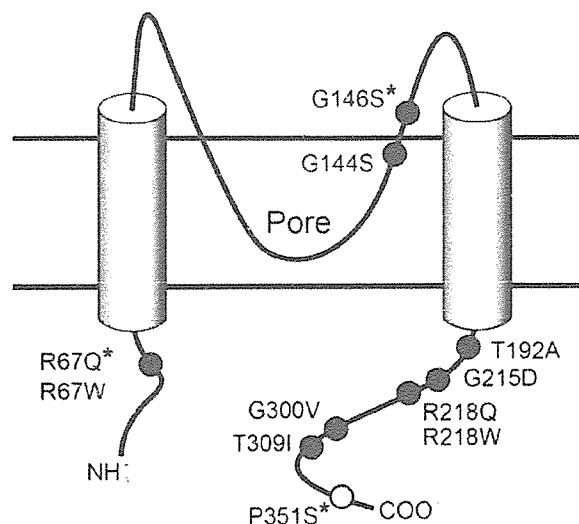
Figure 1. Topology of the Kir 2.1 channel. Scheme showing the topology of the Kir 2.1 channel and the location of 10 *KCNJ2* mutations (filled circles) found in 23 ATS and 1 (open circle) in a LQTS patient. Asterisks indicate novel mutations.

General Clinical Findings

Table 1 summarizes ECG findings and two other major phenotypes in 23 ATS patients. Seven of the 23 mutation carriers (30 %) showed the full clinical triad, and 16 (70 %) had two of the three phenotypes.

Cardiac Manifestations (Table 1 and Fig. 2)

In 2 cases (G146S: a proband, and T309I: a proband), it was difficult to measure the RR interval and recognize the U wave because of very frequent premature contractions and sustained ventricular bigeminy. Two G144S patients had A341V-*KCNQ1* mutation. We therefore excluded these 4 cases from ECG parameter analyses. In the remaining 19 cases, the mean QTc interval was 406 ± 10 ms, and only 3 (16%) had a QTc ≥ 460 ms. Based on the criteria described in Methods, 16 patients (84%) showed abnormal U waves (Fig. 2A-C and Table 1). Their serum K^+ concentrations were within normal range. There were no other factors influencing the U wave formation such as bradycardia or drugs.

Ventricular tachyarrhythmias were observed in 15 patients (65%; 12 of 13 probands and 3 of 10 family members): monomorphic VT in 2 (9%), polymorphic VT in 4 (17%), bidirectional VT in 13 (57%) (Fig. 2D), and ventricular fibrillation (VF) in one (4%).

β blockers (propranolol, atenolol, metoprolol, or carvedilol) were prescribed for 7 individuals, calcium channel blocker (verapamil) for 5 and sodium channel blockers (one is flecainide, the others are mexiletine) for 3. These drugs appeared to prevent cardiac events effectively in each case.

Periodic Paralysis

Periodic paralysis was observed in 13 patients (57%). In some of them, muscle weakness was triggered by elevated fever, exercise, and menstruation. Biopsy of skeletal muscle demonstrated tubular aggregates in 2 probands (Ai, et al., 2002; Hosaka, et al., 2003). Carbonic anhydrase inhibitors prevented or reduced the attack in 4, however, they were not effective in 2 cases.

Table 1

Characteristics of KCNJ2 Mutation Carriers

No of kindred	Mutation in KCNJ2 cDNA	Protein	Age	Sex	HR (bpm)	Cardiac Manifestations QTc (ms)	QUc (ms)	T amplitude (mV)	U amplitude (mV)	Tp-Up (ms)	U/T[††]	Ventricular arrhythmia	Paralysis	Dysmorphology	Symptom	Seizure	Therapy
KJ-01	199C>T	R67W*	30	F	68	383	766	0.60	0.15	240	0.25	a, b, d	-	-	-	-	-
	199C>T	R67W	55	F	71	479	761	0.30	0.15	200	0.50	-	-	+	-	-	-
	199C>T	R67W	20	F	93	430	647	0.15	0.30	200	2.00	b, c	-	+	-	-	-
K-323	200G>A	R67Q*	13	F	54	360	626	1.10	0.30	232	0.27	a, c, d	-	+	Syncope	-	Carvedilol, Mexiletine
K-024	430G>A	G144S*†	36	F	67	480	803	0.40	0.30	280	0.75	a, d, f	-	+	Syncope	-	Propranolol Verapamil +
	430G>A	G144S†	11	M	70	460	756	NA	NA	250	NA	b, d	-	+	Aborted SD	-	Propranolol Verapamil
K-179	436G>A	G146S*	28	F	126[†††]	N	NA	NA	NA	NA	NA	a, b, d, f	+	-	-	-	Atenolol
K-027	574A>G	T192A*	13	M	89	487	731	0.30	0.32	208	1.07	a, b	+	+	-	-	Acetazolamide
	574A>G	T192A	11	F	86	431	790	0.66	0.22	283	0.33	a, f	-	+	-	-	Acetazolamide
N-01	644G>A	G215D*	34	F	73	408	794	0.78	0.33	280	0.42	a, b, f, g	+	+	Aborted SD	-	ICD
K-180	652C>T	R218W*	6	F	80	483	716	0.05	0.15	200	3.00	a, b, c, d, e	-	-	Syncope	+	Flecainide
	652C>T	R218W	38	M	54	384	693	0.80	0.20	250	0.25	e	-	+	-	-	-
	652C>T	R218W	73	M	52	410	670	0.50	0.25	220	0.50	-	+	-	-	-	-
K-240	652C>T	R218W*	11	F	78	365	753	0.30	0.35	240	1.17	b, c, d, e	+	-	-	-	Mexiletine
	652C>T	R218W	47	M	91	394	640	0.45	0.20	240	0.44	-	+	+	-	+	-
	652C>T	R218W	5	M	78	342	684	0.30	0.15	220	0.50	b, c	-	+	Myalgia	-	-
K-324	652C>T	R218W	6	M	82	339	701	0.14	0.20	255	1.43	a, c, d	-	+	-	-	Verapamil
K-178	653G>A	R218Q*	13	F	60	420	700	0.40	0.20	220	0.50	b, c, d	-	+	-	-	-
	653G>A	R218Q	42	M	55	402	651	0.80	0.28	230	0.35	b	+	-	-	-	-
K-201	653G>A	R218Q*	12	F	105	423	741	0.65	0.40	205	0.62	b, c, d	+	-	Palpitation	-	-
K-02	899G>T	G300V*	16	M	103	393	786	0.90	0.30	240	0.33	b, d	+	+	Syncope	-	Propranolol, Verapamil
	899G>T	G300V	36	M	67	444	740	0.45	0.30	240	0.67	a, b, c, d	-	+	Syncope	-	Propranolol K
KJ-03	926C>T	T309I*	17	F	NA	NA	NA	NA	NA	NA	NA	a, b, c, d	+	+	Malaise	-	Metoprolol, Verapamil
			23 ± 31	17	77 ± 41	406 ± 10	715 ± 12	0.51 ± 0.07	0.25 ± 0.02	231 ± 56	0.76 ± 0.16						

Table 1. Characteristics of *KCNJ2* mutation carriers. *: proband. †: compound heterozygous *KCNQ1*(c.1022C>T (p.A341V)) mutation carrier. ††: U/T means the ratio of U amplitude compared to T amplitude. †††: Because this patient had frequent extra ventricular systoles, heart rate was recorded as 126 bpm. NA: nonavailable information. As for ventricular arrhythmias, a: PVC, b: bigeminy, c: couplet, d: bidirectional VT, e: monomorphic VT, f: polymorphic VT, g: VF. SD: sudden cardiac death. As for treatments, K indicates potassium supplement, and ICD: implantable cardioverter defibrillator. The cDNA sequence numbering was based upon GenBank reference sequence NM_000891.2 for *KCNJ2*, NM_000218.2 for *KCNQ1* (the first adenosine in the initiator ATG was designed as +1).

Dysmorphology

Dysmorphology was observed in 17 patients (74%). Mandibular micrognathia (small mandible) was most frequently observed (11; 48%). Short stature was found in 8 (35%); clinodactyly in 6 (26%); hypertelorism in 6 (26%); low-set ears in 5 (22%); broad forehead in 4 (17%); and scoliosis in 1 (4%).

Other Manifestations in ATS Patients

Interestingly, 4 patients (17%) had episodes of afebrile seizures during infancy. Because Kir 2.1 channels are known to be distributed in various types of cells—including major parts of the brain (Raab-Graham, et al., 1994)—seizures as an episodic electrical phenotype of the central nervous system could be a clinical sign of ATS. Mild thyroid dysfunction was observed in one case.
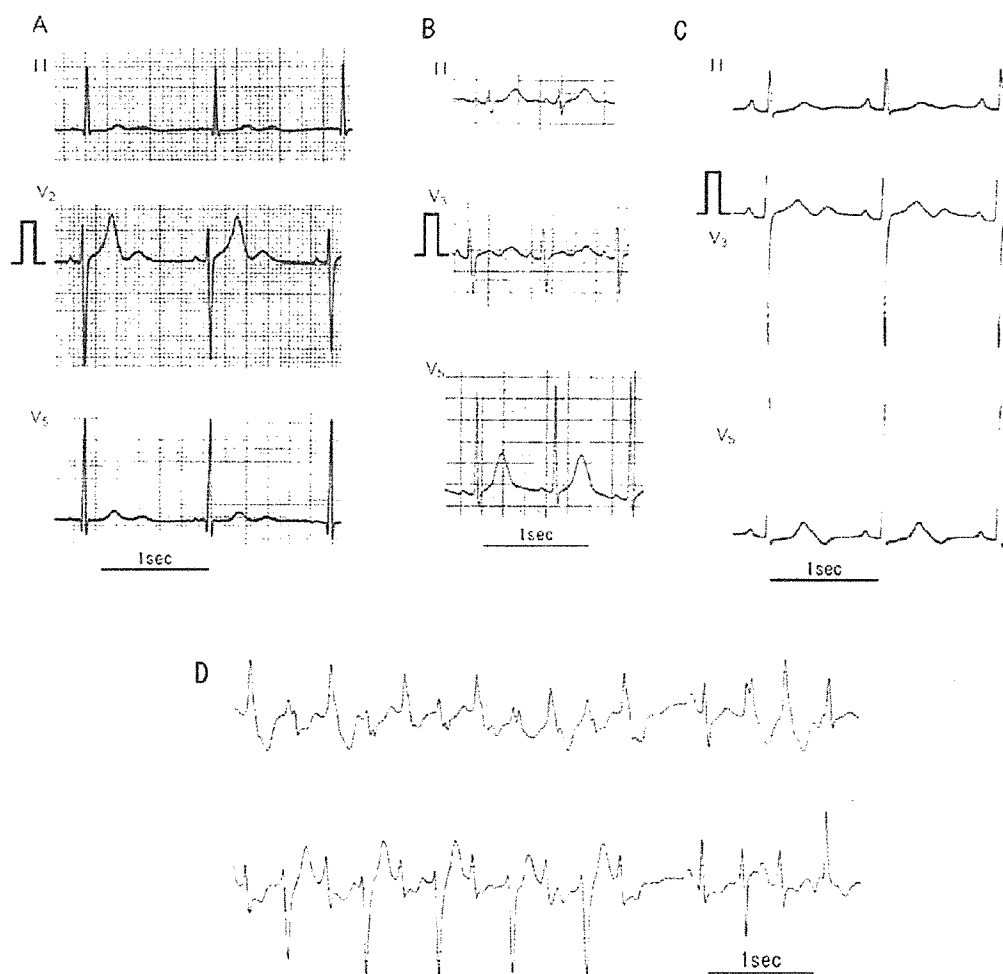

Figure 2. Representative ECG traces of *KCNJ2* mutation carriers. A: Normal QTc (360 ms) and abnormal U wave (U amplitude 0.30 mV) (K-323, R67Q). B: Normal QTc (373 ms) and abnormal U wave (U amplitude 0.30 mV and U amplitude > T amplitude) (KJ-01, R67W). C: QTc prolongation (460 ms) and abnormal U wave (U amplitude 0.30 mV) (K-024, Carrier of compound mutation A341V-*KCNQ1* and G144S-*KCNJ2*). D: bidirectional ventricular tachycardia in a Holter recording (K-179, G146S).

Electrophysiological Functional Assays

R67Q and G146S-*KCNJ2* Channels

We performed biophysical assays for the two novel *KCNJ2* mutations using the whole-cell patch clamp method in COS7 cells.

COS7 cells transfected with WT-*KCNJ2* cDNA (1 μg/dish: Fig. 3A-a) displayed K^+ currents with a strong inward rectification, which are typical of I_{K1} as previously described (Kubo, et al., 1993; Raab-Graham, et al., 1994). However, neither of the mutants—R67Q nor G146S—displayed measurable currents when transfected alone (Fig. 3A-b,c).

To simulate the allelic heterozygosity, WT and each mutant-*KCNJ2* were co-transfected at an equimolar ratio (0.5 μg/dish, respectively, Fig. 3A-d,e). Panel B of Figure 3 shows current-voltage relations. The currents co-expressed of WT with either mutant-*KCNJ2* showed the inward rectification. As summarized in bar graphs of Figure 3C, current densities for co-expression of WT-*KCNJ2* with R67Q (white bar) or G146S (gray bar) were − 123 ± 32 pA/pF and −157 ± 23 pA/pF at −140 mV, and −9 ± 6 pA/pF and −15 ± 5 pA/pF at −50 mV, respectively. They were significantly smaller than those displayed by WT (−362 ± 48 pA/pF at −140 mV and 94 ± 16 pA/pF at − 50 mV, indicated by closed bars). Both mutants showed a larger suppression at −50 mV, which is more physiological membrane potential.
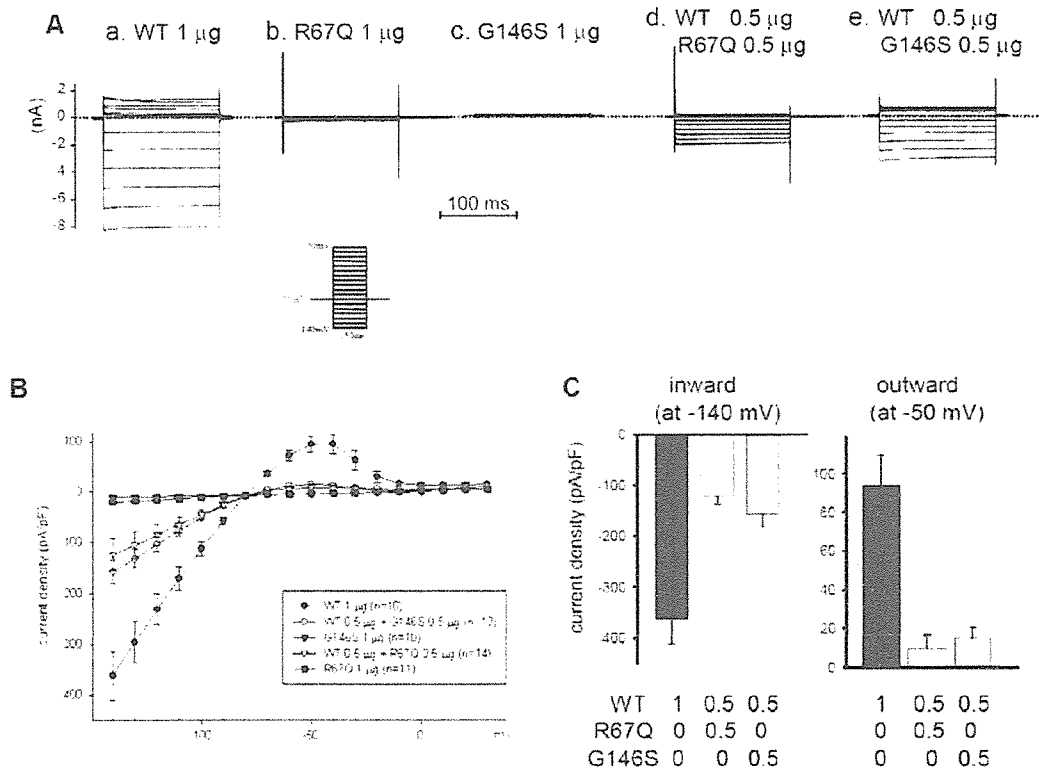

Figure 3. Both R67Q-*KCNJ2* and G146S-*KCNJ2* exert dominant negative effects on wild type function. A: Representative Kir 2.1 currents expressed in COS7 cells: (a) wild type (WT) cDNA 1 μg, (b) R67Q 1 μg, (c) G146S 1 μg, (d) co-transfection with WT 0.5 μg and R67Q 0.5 μg and (e) co-transfection with WT 0.5 μg and G146S 0.5 μg. Holding potential was set at −80 mV. Square pulses of 150 ms duration were applied to the potentials between −140 mV and +30 mV with a 10 mV increment. Time scale is given in the middle of graph. B: Plots for current-voltage relationships obtained by multiple experiments of the same protocol as shown in A. Current densities were calculated by dividing with cell capacitance. C: Bar graphs showing mean current densities in WT (black bars), co-transfection with WT and R67Q

(white bars) and co-transfection with WT and G146S (gray bars); left panel: those at −140 mV and right panel: those at −50 mV. Vertical bars indicate SEM.

P351S-*KCNJ2* Channel

We found one novel *KCNJ2*-variant (P351S) among 74 LQTS probands (1.4%). Functional assays revealed that the mutant channel displayed inwardly rectifying currents of similar size (Fig. 4A). In a heterozygous condition (Fig. 4B), the current densities of WT and WT/P351S were −362 ± 48 pA/pF and −350 ± 38 pA/pF at −140 mV, and 90 ± 15 pA/pF and 94 ± 20 pA/pF at −50 mV, respectively. Student *t*-tests revealed these changes in current were not significant. These findings suggested that the P351S-*KCNJ2* was a non-pathological variant associated with the LQT1 patient who lacked extra-cardiac signs of ATS.
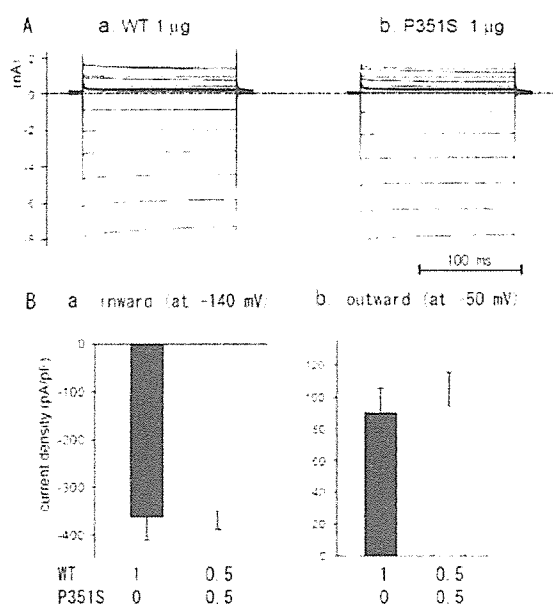

Figure 4. The Kir 2.1 variant in LQTS displays inwardly rectifying currents, which are indistinguishable from that of the WT. A: Representative Kir 2.1 currents expressed in COS7 cells: (a) WT cDNA 1 µg, (b) P351S 1 µg. Pulse protocols were the same in Fig. 3. B: Bar graphs showing averaged current densities induced by WT (black) and co-transfection of WT/P 351S (white) at test of (a) −140 mV and (b) −50 mV (n=8 respectively).

Immunocytochemistry of Mutant Channels (R67Q and G146S)

In order to investigate whether the R67Q and G146S mutations affect *KCNJ2* trafficking, immunocytochemistry and confocal imaging of mutant channels was performed. An HA tag was introduced into an extracellular loop lesion of *KCNJ2* in the pCMS-EGFP vector which carried GFP as a reporter gene. The HA-tagging procedure itself did not affect the functional expression of inwardly rectifying I_{K1} currents (data not shown).

Figure 5 illustrates typical results of confocal imaging. COS7 cells were transfected with HA-*KCNJ2*, HA-R67Q, HA-G146S and *KCNJ2* (without HA tag)(Fig 5, upper panel). All of HA-tagged *KCNJ2* (HA-*KCNJ2*, HA-R67Q and HA-G146S) exhibited red fluorescence at the plasma membrane (Fig 5, middle panel), indicating that both R67Q and G146S were trafficking-competent mutants.
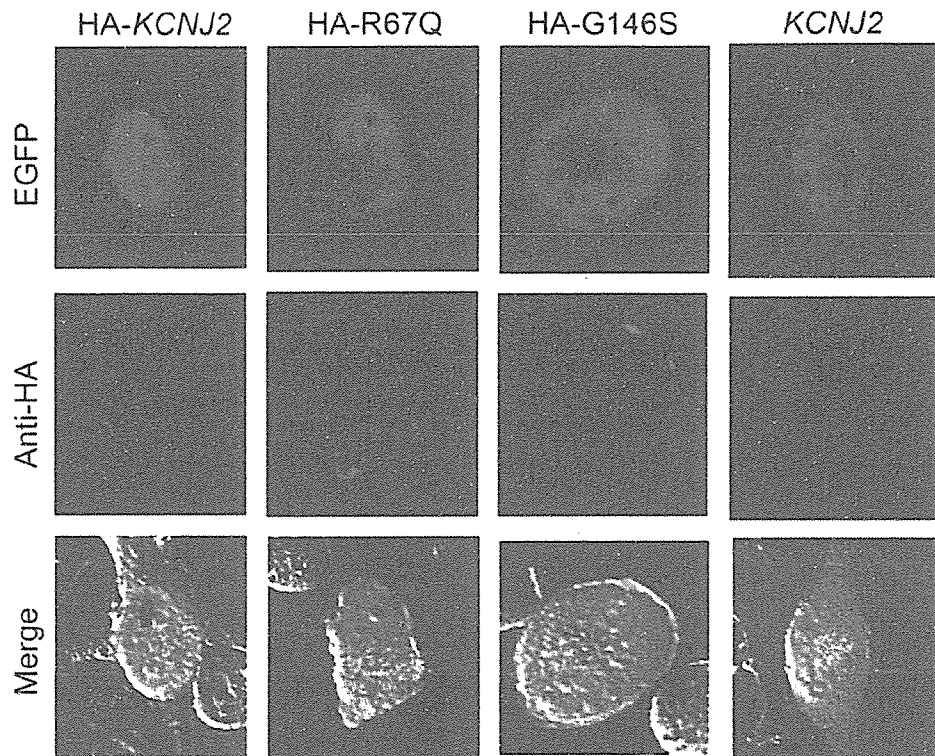
Figure 5. Cellular localization of WT and mutant Kir 2.1 channels. In figure, HA-*KCNJ2* indicates HA-tagged WT-*KCNJ2* (positive control), *KCNJ2*; WT-*KCNJ2* without HA tagging (negative control), and HA-R67Q and HA-G146S; HA-tagged mutant *KCNJ2*. Upper panel shows green fluorescence of GFP, middle panel; red fluorescence of secondary anti-HA antibody, bottom panel; merge of green fluorescence, red fluorescence, and transmission.

DISCUSSION

ATS is a rare inherited disorder characterized by periodic paralysis, mild dysmorphic features, and QT or QU prolongation with ventricular arrhythmias in ECGs. Mutations of *KCNJ2* have been identified in patients with ATS (ATS1). However, about 20-30% of clinically diagnosed ATS patients do not have the *KCNJ2* mutation (Plaster, et al., 2001; Tristani-Firouzi, et al., 2002; Zhang, et al., 2005), suggesting genetic heterogeneity. In the present study, we screened 23 clinically diagnosed ATS patients and identified 10 variations of *KCNJ2* mutations (including 2 novels, R67Q and G146S). Every genotyped patient had one of these 10 mutations. Therefore, all were ATS1 patients. As in our study, a recent genetic survey conducted in the UK (Davies, et al., 2005) demonstrated that all 11 probands from 11 unrelated ATS families were *KCNJ2*-positive (100% ATS1). Our findings, along with that of the UK, seem to contradict the prevalence rate mentioned above, however, ATS is a rare disorder and we should await future studies.

With regard to the cardiac manifestation of ATS, the mean QTc interval was within normal range (406 ± 10 ms), and only 3 of 19 cases (16%) showed prolonged QT intervals. In contrast, abnormal U waves were present in the majority (80%), thereby causing a markedly prolonged QUc interval (715 ± 12 ms). Although ATS had been suggested as a subtype of LQTS (LQT7), Zhang et al. showed the median QTc interval was within the normal range in 96 *KCNJ2*-positive ATS patients and suggested that the QTc prolongation reported in earlier studies was

due to the inclusion of U waves in the QT measurement. Our study supported their conclusion, and *KCNJ2*-positive ATS should be classified as ATS1 but not LQT7. In most patients, QTc intervals were within normal range, and the QTc prolongation was observed in only 3 pure ATS patients and 2 ATS patients with compound *KCNQ1* mutation (K-024) (Data of these two compound mutation patients were not included in the analysis of ECG parameters as described above). In our study, if cardiac manifestations were defined as abnormal U waves and/or ventricular arrhythmias, the penetration of cardiac manifestations was up to 96% (22 of 23).

The clinical severity of ventricular arrhythmias was reported to be milder in ATS than other subtypes of LQTS (Plaster, et al., 2001); however, 2 unrelated patients in our cohort experienced aborted sudden death (Hosaka, et al., 2003; Kobori, et al., 2004). Aborted sudden deaths have also been reported in the past (Junker, et al., 2002). It is much too early to conclude that arrhythmias in ATS are, for the most part, benign. Further studies are required to determine long-term prognosis, risk stratification for life threatening cardiac phenotypes, and for effective treatment.

Afebrile seizures were noted during infancy in 4 of 23 ATS patients (17%). This episodic electrical disorder related to the central nervous system was previously reported in one ATS patient having tonic clonic seizures associated with vomiting (Canun, et al., 1999). In our patients with a history of seizures, there were no identified fundamental conditions, including elevated fever, electrolyte abnormality, and/or organic central nervous system disorders. As for a possible mechanism underlying the seizures, Neusch and coworkers (Neusch, et al., 2003) demonstrated that reduced K^+ conductance induced by Kir mutants would disturb the clearance of external K^+ by glial cells during neuronal activities. Therefore, the impaired spatial K^+ buffering induced stronger and prolonged depolarization of glial cells and neurons in response to activity-dependent K^+ release, which may generate the seizures. Furthermore, the Kir current density has been noted to be reduced in temporal lobe epilepsy (Bordey and Sontheimer, 1998; Schroder, et al., 2000). It remains, however, unknown why these patients experienced the seizures only during infancy.

Subsequent functional assays for novel *KCNJ2* mutations (R67Q and G146S) revealed that they were non-functional and trafficking-competent mutations. In a heterozygous condition, they both caused strong dominant negative suppression effects (91% and 84% reduction at −50 mV respectively) (Fig. 3). These biophysical properties may be compatible with pathological roles in expression of ATS phenotypes as well as other mutations previously reported (Lange, et al., 2003).

In conclusion, Japanese ATS patients were exclusively associated with *KCNJ2* mutations (100% ATS1) and presented a high penetrance of cardiac manifestations (96%). ATS1 is a disorder distinct from LQTS. The disease entity is more characterized by a normal QTc interval, abnormal U waves and ventricular arrhythmias, typically bidirectional VT.

REFERENCES

Ai T, Fujiwara Y, Tsuji K, Otani H, Nakano S, Kubo Y, Horie M. 2002. Novel KCNJ2 mutation in familial periodic paralysis with ventricular dysrhythmia. Circulation 105(22):2592-4.

Andelfinger G, Tapper AR, Welch RC, Vanoye CG, George AL, Jr., Benson DW. 2002. KCNJ2 mutation results in Andersen syndrome with sex-specific cardiac and skeletal muscle phenotypes. Am J Hum Genet 71(3):663-8.

Andersen ED, Krasilnikoff PA, Overvad H. 1971. Intermittent muscular weakness, extrasystoles, and multiple developmental anomalies. A new syndrome? Acta Paediatr Scand 60(5):559-64.

Ballester LY, Benson DW, Wong B, Law IH, Mathews KD, Vanoye CG, George AL, Jr. 2006. Trafficking-competent and trafficking-defective KCNJ2 mutations in Andersen syndrome. Hum Mutat 27(4):388.

Bazzett HC. 1920. An analysis of the time relationships or time-relations of electrocardiograms. Heart 7:353-380.

Bendahhou S, Fournier E, Sternberg D, Bassez G, Furby A, Sereni C, Donaldson MR, Larroque MM, Fontaine B, Barhanin J. 2005. In vivo and in vitro functional characterization of Andersen's syndrome mutations. J Physiol 565(Pt 3):731-41.

Bordey A, Sontheimer H. 1998. Properties of human glial cells associated with epileptic seizure foci. Epilepsy Res 32(1-2):286-303.

Canun S, Perez N, Beirana LG. 1999. Andersen syndrome autosomal dominant in three generations. Am J Med Genet 85(2):147-56.

Davies NP, Imbrici P, Fialho D, Herd C, Bilsland LG, Weber A, Mueller R, Hilton-Jones D, Ealing J, Boothman BR and others. 2005. Andersen-Tawil syndrome: new potassium channel mutations and possible phenotypic variation. Neurology 65(7):1083-9.

Donaldson MR, Jensen JL, Tristani-Firouzi M, Tawil R, Bendahhou S, Suarez WA, Cobo AM, Poza JJ, Behr E, Wagstaff J and others. 2003. PIP2 binding residues of Kir2.1 are common targets of mutations causing Andersen syndrome. Neurology 60(11):1811-6.

Doyle DA, Morais Cabral J, Pfuetzner RA, Kuo A, Gulbis JM, Cohen SL, Chait BT, MacKinnon R. 1998. The structure of the potassium channel: molecular basis of K+ conduction and selectivity. Science 280(5360):69-77.

Hosaka Y, Hanawa H, Washizuka T, Chinushi M, Yamashita F, Yoshida T, Komura S, Watanabe H, Aizawa Y. 2003. Function, subcellular localization and assembly of a novel mutation of KCNJ2 in Andersen's syndrome. J Mol Cell Cardiol 35(4):409-15.

Junker J, Haverkamp W, Schulze-Bahr E, Eckardt L, Paulus W, Kiefer R. 2002. Amiodarone and acetazolamide for the treatment of genetically confirmed severe Andersen syndrome. Neurology 59(3):466.

Keating M, Atkinson D, Dunn C, Timothy K, Vincent GM, Leppert M. 1991. Linkage of a cardiac arrhythmia, the long QT syndrome, and the Harvey ras-1 gene. Science 252(5006):704-6.

Kobori A, Sarai N, Shimizu W, Nakamura Y, Murakami Y, Makiyama T, Ohno S, Takenaka K, Ninomiya T, Fujiwara Y and others. 2004. Additional gene variants reduce effectiveness of beta-blockers in the LQT1 form of long QT syndrome. J Cardiovasc Electrophysiol 15(2):190-9.

Kubo Y, Baldwin TJ, Jan YN, Jan LY. 1993. Primary structure and functional expression of a mouse inward rectifier potassium channel. Nature 362(6416):127-33.

Kubota T, Shimizu W, Kamakura S, Horie M. 2000. Hypokalemia-induced long QT syndrome with an underlying novel missense mutation in S4-S5 linker of KCNQ1. J Cardiovasc Electrophysiol 11(9):1048-54.

Lange PS, Er F, Gassanov N, Hoppe UC. 2003. Andersen mutations of KCNJ2 suppress the native inward rectifier current IK1 in a dominant-negative fashion. Cardiovasc Res 59(2):321-7.

Lepeschkin E. 1969. The U wave of the electrocardiogram. Mod Concepts Cardiovasc Dis 38(8):39-45.

Lepeschkin E. 1972. Physiologic basis of the U wave. New York: Grune and Stratton.

McManis PG, Lambert EH, Daube JR. 1986. The exercise test in periodic paralysis. Muscle Nerve 9(8):704-10.

Neusch C, Weishaupt JH, Bahr M. 2003. Kir channels in the CNS: emerging new roles and implications for neurological diseases. Cell Tissue Res 311(2):131-8.

Ning L, Moss A, Zareba W, Robinson J, Rosero S, Ryan D, Qi M. 2003. Denaturing high-performance liquid chromatography quickly and reliably detects cardiac ion channel mutations in long QT syndrome. Genet Test 7(3):249-53.

Plaster NM, Tawil R, Tristani-Firouzi M, Canun S, Bendahhou S, Tsunoda A, Donaldson MR, Iannaccone ST, Brunt E, Barohn R and others. 2001. Mutations in Kir2.1 cause the developmental and episodic electrical phenotypes of Andersen's syndrome. Cell 105(4):511-9.

Raab-Graham KF, Radeke CM, Vandenberg CA. 1994. Molecular cloning and expression of a human heart inward rectifier potassium channel. Neuroreport 5(18):2501-5.

Sansone V, Griggs RC, Meola G, Ptacek LJ, Barohn R, Iannaccone S, Bryan W, Baker N, Janas SJ, Scott W and others. 1997. Andersen's syndrome: a distinct periodic paralysis. Ann Neurol 42(3):305-12.

Schroder W, Hinterkeuser S, Seifert G, Schramm J, Jabs R, Wilkin GP, Steinhauser C. 2000. Functional and molecular properties of human astrocytes in acute hippocampal slices obtained from patients with temporal lobe epilepsy. Epilepsia 41 Suppl 6:S181-4.

Tawil R, Ptacek LJ, Pavlakis SG, DeVivo DC, Penn AS, Ozdemir C, Griggs RC. 1994. Andersen's syndrome: potassium-sensitive periodic paralysis, ventricular ectopy, and dysmorphic features. Ann Neurol 35(3):326-30.

Tristani-Firouzi M, Jensen JL, Donaldson MR, Sansone V, Meola G, Hahn A, Bendahhou S, Kwiecinski H, Fidzianska A, Plaster N and others. 2002. Functional and clinical characterization of KCNJ2 mutations associated with LQT7 (Andersen syndrome). J Clin Invest 110(3):381-8.

Yan GX, Antzelevitch C. 1998. Cellular basis for the normal T wave and the electrocardiographic manifestations of the long-QT syndrome. Circulation 98(18):1928-36.

Yoshida H, Horie M, Otani H, Takano M, Tsuji K, Kubota T, Fukunami M, Sasayama S. 1999. Characterization of a novel missense mutation in the pore of HERG in a patient with long QT syndrome. J Cardiovasc Electrophysiol 10(9):1262-70.

Zhang L, Benson DW, Tristani-Firouzi M, Ptacek LJ, Tawil R, Schwartz PJ, George AL, Horie M, Andelfinger G, Snow GL and others. 2005. Electrocardiographic features in Andersen-Tawil syndrome patients with KCNJ2 mutations: characteristic T-U-wave patterns predict the KCNJ2 genotype. Circulation 111(21):2720-6.

ELSEVIER

Original article

Mechanistic basis for the pathogenesis of long QT syndrome associated with a common splicing mutation in KCNQ1 gene

Keiko Tsuji [a,c,d], Masaharu Akao [a,*], Takahiro M. Ishii [b], Seiko Ohno [a], Takeru Makiyama [a], Kotoe Takenaka [a], Takahiro Doi [a], Yoshisumi Haruna [a], Hidetada Yoshida [a], Toshihiro Nakashima [c], Toru Kita [a], Minoru Horie [d]

[a] Department of Cardiovascular Medicine, Kyoto University Graduate School of Medicine, 54 Kawahara-cho, Shogoin, Sakyo-ku, Kyoto 606-8507, Japan
[b] Department of Physiology, Kyoto University Graduate School of Medicine, Japan
[c] Department of Applied Biology, Kyoto Institute of Technology, Kyoto, Japan
[d] Department of Cardiovascular and Respiratory Medicine, Shiga University of Medical Science, Japan

Abstract

Mutations in KCNQ1, the gene encoding the delayed rectifier K⁺ channel in cardiac muscle, cause long QT syndrome (LQTS). We studied 3 families with LQTS, in whom a guanine to adenine change in the last base of exon 7 (c.1032G>A), previously reported as a common splice-site mutation, was identified. We performed quantitative measurements of exon-skipping KCNQ1 mRNAs caused by this mutation using real-time reverse transcription polymerase chain reaction. Compared with normal individuals who have minor fractions of splicing variants (Δ7–8: 0.1%, Δ8: 6.9%, of total KCNQ1 transcripts), the affected individuals showed remarkable increases of exon-skipping mRNAs (Δ7: 23.5%, Δ7–8: 16.8%, Δ8: 4.5%). Current recordings from *Xenopus laevis* oocytes heterologously expressing channels of wild-type (WT) or exon-skipping KCNQ1 (Δ7, Δ7–8, or Δ8) revealed that none of the mutants produced any measurable currents, and moreover they displayed mutant-specific degree of dominant-negative effects on WT currents, when co-expressed with WT. Confocal microscopy analysis showed that fluorescent protein-tagged WT was predominantly expressed on the plasma membrane, whereas the mutants showed intracellular distribution. When WT was co-expressed with mutants, the majority of WT co-localized with the mutants in the intracellular space. Finally, we provide evidence showing direct protein–protein interactions between WT and the mutants, by using fluorescence resonance energy transfer. Thus, the mutants may exert their dominant-negative effects by trapping WT intracellularly and thereby interfering its translocation to the plasma membrane. In conclusion, our data provide a mechanistic basis for the pathogenesis of LQTS caused by a splicing mutation in KCNQ1.
© 2007 Elsevier Inc. All rights reserved.

Keywords: Potassium channels; Arrhythmia; Long QT syndrome; Mutation; Splicing

1. Introduction

Long QT syndrome (LQTS) is characterized by prolongation of the cardiac action potential, syncopal attacks, torsades de pointes arrhythmias, and sudden cardiac death [1–3]. The slow component of delayed rectifier K⁺ current (I_{Ks}) in the heart modulates repolarization of cardiac action potential. The I_{Ks} channel is formed by the co-assembly of KCNQ1 α-subunits and KCNE1 β-subunits [4,5]. Mutations in the KCNQ1 cause the most frequent form of inherited LQTS [6]. We studied 3 families

with LQTS, in whom a guanine to adenine change in the last base of exon 7 (c.1032G>A) of KCNQ1 was identified. Among our entire group of KCNQ1-related LQTS patients, the frequency of this mutation was remarkably high (we found this mutation in 3 out of 22 families with KCNQ1 mutations, among a total of 185 families with LQTS), in agreement with the previous report that this is a mutation "hot-spot" [7]. Mutations at this spot (c.1032G>A or c.1032G>C), which do not alter the coded alanine (A344A), have been considered to act as splice mutations in KCNQ1, by altering the intron 7 donor splice-site consensus sequence [8,9]. Murray et al. [7] demonstrated the presence of exon-skipping transcripts (with loss of exon 8 (Δ8) or of exon 7–8 (Δ7–8)) in peripheral blood leukocytes of

* Corresponding author. Tel.: +81 75 751 3194; fax: +81 75 751 4284.
E-mail address: akao@kuhp.kyoto-u.ac.jp (M. Akao).